# Bioluminescence Resonance Energy Transfer Assays Reveal Ligand-specific Conformational Changes within Preformed Signaling Complexes Containing δ-Opioid Receptors and Heterotrimeric G Proteins*□S

**Nicolas Audet**[‡§¶], **Céline Galés**[∥], **Élodie Archer-Lahlou**[‡§¶1], **Marc Vallières**[‡], **Peter W. Schiller**[§**], **Michel Bouvier**[¶‡‡2], **and Graciela Pineyro**[‡§¶§§3]

From the ‡Centre de Recherche Fernand-Seguin, Hôpital Louis-H. Lafontaine, Montréal, Quebec H1N 3V2, Canada, the §Département de Pharmacologie, ‡‡Département de Biochimie, and §§Département de Psychiatrie, Faculté de Médecine, Université de Montréal, Montréal, Quebec H3C 3J7, Canada, ¶Groupe de Recherche Universitaire sur le Médicament, Montréal, Quebec H3C 3J7, Canada, ∥INSERM Unité 858, Équipe 8, Institut Louis Bugnard, Toulouse 31432, France, and **Laboratory of Chemical Biology and Peptide Research, Institut de Recherches Cliniques de Montréal, Montréal, Quebec 2W 1R7, Canada

Heptahelical receptors communicate extracellular information to the cytosolic compartment by binding an extensive variety of ligands. They do so through conformational changes that propagate to intracellular signaling partners as the receptor switches from a resting to an active conformation. This active state has been classically considered unique and responsible for regulation of all signaling pathways controlled by a receptor. However, recent functional studies have challenged this notion and called for a paradigm where receptors would exist in more than one signaling conformation. This study used bioluminescence resonance energy transfer assays in combination with ligands of different functional profiles to provide *in vivo* physical evidence of conformational diversity of δ-opioid receptors (DORs). DORs and $\alpha_{i1}\beta_1\gamma_2$ G protein subunits were tagged with Luc or green fluorescent protein to produce bioluminescence resonance energy transfer pairs that allowed monitoring DOR-G protein interactions from different vantage points. Results showed that DORs and heterotrimeric G proteins formed a constitutive complex that underwent structural reorganization upon ligand binding. Conformational rearrangements could not be explained by a two-state model, supporting the idea that DORs adopt ligand-specific conformations. In addition, conformational diversity encoded by the receptor was conveyed to the interaction among heterotrimeric subunits. The existence of multiple active receptor states has implications for the way we conceive specificity of signal transduction.

Heptahelical receptors are versatile membrane proteins that play an important role in cellular communication. They do so by recognizing a large variety of extracellular ligands that convey information to the intracellular compartment by modifying receptor conformation upon binding. These structural modifications then trigger an array of biochemical changes that ultimately control vital processes within the cell. Traditionally, conformational changes induced by ligand binding have been thought to shift equilibrium between an active and an inactive conformation of the receptor. According to this classical view, all agonists would stabilize a single active state that equally effectively stimulates all signaling pathways controlled by the receptor (1). In consequence, ligand ability to stabilize this unique active state would be the only determinant of ligand efficacy at all functional readouts. Furthermore, this model predicts that ligand rank order of efficacy across different readouts should be maintained, representing a progressive accumulation (or decrease) of the single active state of the receptor (2).

However, recent data have challenged this view, suggesting that the complexity of heptahelical receptor signaling cannot be based on the accumulation of a single active receptor conformation, and efficacy cannot be restricted to only a quantitative dimension (3, 4). Evidence supporting this assertion has been largely based on functional studies whose results cannot be adequately rationalized by accumulation of a single active state but are intuitively explained by assuming the existence of conformational diversity among active forms of the receptor (4). In particular, these studies show that agonists acting at the same receptor may display a different rank order of efficacies when tested at different functional readouts (5–7). In addition to this indirect body of evidence, the possibility that different agonists may stabilize different conformations of the same receptor is supported by *in vitro* physical data. In particular, fluorescence and spectroscopy approaches have confirmed that ligands of different efficacies impose distinct structural constraints upon

purified $\beta 2$-adrenergic receptors, DORs,[4] and muscarinic receptors (8–10). The problem with these observations is that they have not allowed us to establish if ligand-specific receptor states exist in living cells and, if so, whether these different conformations may be discriminated by postreceptor signaling partners.

In the present study, we sought to determine whether DORs occupied by different ligands would differ in the way they interact with heterotrimeric G proteins, the rationale being that if DORs were stabilized in ligand-specific conformations, then each of these receptor states should distinctively interact with its immediate signaling partners. Interaction between DORs and $\alpha\beta\gamma$ subunits was assessed using BRET assays, a technology that has been validated to study not only *in vivo* coupling of heptahelical receptors to $\alpha\beta\gamma$ subunits (11, 12) but to monitor *in vivo* intermolecular interactions within the G protein heterotrimer (13, 14). Results showed that DORs and $\alpha_1\beta_1\gamma_2$ subunits formed a constitutive complex, and BRET assays demonstrated that conformational changes imposed by different ligands were compatible with a multistate rather than a two-state model.

## EXPERIMENTAL PROCEDURES

*Reagents*—Buffer chemicals, protease inhibitors, DPDPE, morphine, naloxone, forskolin, 3-isobutyl-1-methylxanthine, PTX, anti-FLAG M2 affinity resin, and FLAG peptide were purchased from Sigma. [$^{35}$S]GTP$\gamma$S, [$^3$H]adenosine, and coelanterazine were from PerkinElmer Life Sciences. SNC-80 was from Tocris Cookson, and TIPP and TICP were synthesized as previously described (15). G418, Dulbecco's modified Eagle's medium, fetal bovine serum, glutamine, penicillin, and streptomycin were purchased from Wisent.

*DNA Constructs*—Recombinant plasmids encoding for $\alpha_{i1}$-Luc constructs were prepared as previously described (14), using flexible linkers (SGGGGS) to insert the coding sequence of humanized *Renilla* luciferase (*R*Luc; PerkinElmer Life Sciences) into the coding sequence of human $G\alpha_{i1}$, either between residues Gly$^{60}$ and Tyr$^{61}$ ($G\alpha_{i1}$-60*R*luc), Leu$^{91}$ and Lys$^{92}$ ($G\alpha_{i1}$-91*R*luc), or Glu$^{122}$ and Leu$^{123}$ ($G\alpha_{i1}$-122*R*luc). The plasmid encoding $\gamma_2$ with green fluorescent protein (GFP10) fused to its N terminus (11) and vectors encoding FLAG, GFP2, and *R*Luc fused in frame at the C terminus of human DORs have been previously described (16). Generation of CD8-GFP2 and CD8-*R*Luc has also been reported (11, 14).

*Cell Culture and Expression of Heterologous Proteins*—HEK293 cells were cultured in Dulbecco's modified Eagle's medium supplemented with 5% fetal bovine serum and 2 nM L-glutamine. For transient expression of recombinant proteins, cells were seeded at a density of $3 \times 10^6$ cells in 100-mm Petri dishes, cultured for 24 h, and then transfected with vectors encoding BRET constructs for DORs and different G protein subunits along with untagged complementary heterotrimeric

components. Transfections were done using FuGENE 6 reagent (Roche Applied Science) according to the manufacturer's protocol. Titration BRET assays were done as previously described (11), using a fixed amount of donor-tagged proteins (*R*Luc) that was co-expressed with increasing amounts of vector coding for the acceptor (GFP). Untagged subunits complementary to G protein BRET constructs were also included, at DNA levels that would support membrane expression of the heterotrimer at all points of the titration curve. Titration curves allowed us to determine the relative amount of DNA constructs necessary to achieve a maximal BRET signal that was then used in transfections for single point assays. Forty-eight hours after transfection, cells were used in BRET, cyclase, or immunopurification assays. Clones stably expressing FLAG-tagged human DORs were generated as previously described (17) and transiently transfected with $\alpha_{i1}$-Luc·GFP-$\gamma_2$ along with untagged $\beta 1$ subunits.

*BRET Measurements*—Forty-eight hours after transfection, cells were washed twice and mechanically detached with phosphate-buffered saline and centrifuged 5 min at $300 \times g$, followed by resuspension in phosphate-buffered saline. Cells were then distributed into a 96-well microplate (white Optiplate; PerkinElmer Life Sciences) at a concentration of 50,000–100,000 cells/well, which allowed us to achieve luminescence levels suitable for BRET readings using different constructs. Treatments and BRET readings were done according to a previously established protocol that was optimized for assessing *in vivo* ligand effects on receptor interaction with heterotrimeric G proteins (11, 14). Briefly, intact living cells were suspended in phosphate-buffered saline, kept at room temperature, and incubated in the presence or absence of different ligands for 2 min, followed by the addition of the *R*luc substrate, DeepBlueC coelenterazine (PerkinElmer Life Sciences) at a final concentration of 5 $\mu$M. Readings were obtained 2 min after coelanterazine addition, using a modified top count apparatus (TopCount NXT™; PerkinElmer Life Sciences) that allows the sequential integration of the signals detected in the 370–450 and 500–530 nm windows using filters with the appropriate band pass (Chroma). The BRET2 signal was determined by calculating the ratio of the light emitted by GFP2·GFP10 (500–530 nm) over the light emitted by the *R*luc (370–450 nm). BRET2 values were corrected by subtracting the BRET background signal (detected when the *R*luc-tagged construct was expressed alone) from the BRET signal detected in cells coexpressing both Rluc- and GFP (net BRET).

For titration experiments, the expression level of each tagged protein was determined by direct measurement of total fluorescence and luminescence on aliquots of the transfected cells. Total fluorescence was measured using a FluoroCount (PerkinElmer) with an excitation filter at 400 nm and an emission filter at 510 nm and the following parameters: gain, 1; photomultiplier tube, 1100 V; time, 1.0 s. After measuring fluorescence, the same cell samples were incubated with coelenterazine h (5 $\mu$M; 8 min; Nanolight Technology), and total cell luminescence was measured using a LumiCount (PerkinElmer Life Sciences) with the following parameters: gain, 1; photomultiplier tube, 900 V; time, 1 s.

*Immunopurification Assays and Western Blot Analysis*—Cells were recovered in phosphate-buffered saline and treated

---

[4] The abbreviations used are: DOR, $\delta$-opioid receptor; BRET, bioluminescence resonance energy transfer; *R*Luc, *Renilla* luciferase; DPDPE, D-pen-2,5-enkephalin; TIPP, Tyr-L-1,2,3,4-tetrahydroisoquinoline-3-carboxylic acid-Phe-Phe-OH; TICP$\Psi$, Tyr-Tic$\Psi$[CH$_2$NH]cyclohexylalanine-Phe-OH; ERK, extracellular signal-regulated kinase; pERK, phospho-ERK; GFP, green fluorescent protein; PTX, pertussis toxin; GTP$\gamma$S, guanosine 5′-3-O-(thio)triphosphate.

with DPDPE or TICP (10 $\mu$M, 5 min) as described above. Following treatment, cells were suspended in lysis buffer (5 mM Tris, 3 mM MgCl$_2$, 2 mM EDTA, 1 mM NaF, 1 mM Na$_3$VO$_4$, 5 $\mu$g/ml leupeptin, 5 $\mu$g/ml soybean trypsin inhibitor, and 10 $\mu$g/ml benzamidine) and homogenized using an Ultraturax homogenizer (IKA, Wilmington, NC). Following centrifugation at $300 \times g$ for 5 min, the supernatant was centrifuged at $30,000 \times g$ for 20 min, and the resultant pellet was resuspended in lysis buffer for a second round of centrifugation ($30,000 \times g$; 20 min). The pellet obtained was then solubilized in 0.5% *n*-dodecylmaltoside, 25 mM Tris, pH 7.4, 140 mM NaCl, 2 mM EDTA, 1 mM NaF, 1 mM Na$_3$VO$_4$, 5 $\mu$g/ml leupeptin, 5 $\mu$g/ml soybean trypsin inhibitor, and 10 $\mu$g/ml benzamidine. Following agitation at 4 °C for 2 h, the solubilized fraction was centrifuged at $10,000 \times g$ for 30 min, and the receptor was immunopurified from the supernatant fraction using an anti-FLAG M2 antibody resin. 20 $\mu$l of antibody-coupled resin equilibrated in solubilization buffer and supplemented with 0.1% bovine serum albumin (w/v) were used to purify the receptor overnight at 4 °C under gentle agitation. The next morning, the resin was pelleted and washed twice with 500 $\mu$l of solubilization buffer and four times with 500 $\mu$l of modified solubilization buffer (containing 0.1% instead of 0.5% *n*-dodecyl-maltoside (w/v)). The receptor was then eluted by incubating the resin for 10 min at 4 °C with 100 $\mu$l of modified solubilization buffer containing a FLAG peptide (150 $\mu$g/ml). This elution was repeated three times, and the eluates were combined and concentrated by membrane filtration over Microcon-30 concentrators (Millipore). SDS sample buffer was then added, and samples were used for SDS-PAGE. SDS-PAGE was performed using a 4% stacking gel and 10% separating gel. Proteins resolved in SDS-PAGE were then transferred (50 mA, 16 h; Bio-Rad Mini-Trans Blot apparatus) from gels onto nitrocellulose (GE Healthcare). The amount of endogenous or Luc-tagged G$\alpha_{i1}$ or G$\beta$ that was recovered with immunopurified DORs was assessed using 1:1000 polyclonal antibodies raised against G$\alpha_{i1}$ or G$\beta$, followed by secondary anti-rabbit horseradish-conjugated antibodies (1:40,000; Amersham Biosciences). The total amount of receptor loaded for each sample was detected by probing the samples with anti-FLAG M2 antibody (1:5000), followed by secondary anti-mouse horseradish-conjugated antibodies (1:40,000; Amersham Biosciences).

*cAMP Accumulation Assays*— cAMP accumulation assays were carried out according to a previously described protocol (18), and [$^3$H]ATP and [$^3$H]cAMP were separated by sequential chromatography on Dowex exchange resin and aluminum oxide columns. cAMP produced was estimated by calculating the ratio of [$^3$H]cAMP/[$^3$H]ATP plus [$^3$H]cAMP in each sample.

*[$^{35}$S]GTP$\gamma$S Binding Assays*—The procedure for [$^{35}$S]GTP$\gamma$S binding has been detailed in a previous report (18).

*Data Analysis*—Statistical comparisons were done by one-way analysis of variance using Dunnett's correction to compare drug effects with basal conditions and Fisher's "least significance difference" adjustment in order to assess differences among drugs. Modification of drug effects by PTX was analyzed by covariance using basal values as co-regressor. Except for Fig. 2, all figures present data as differences or percentage changes

with respect to basal, but in all cases statistical analyses were carried out on raw net BRET ratio, cAMP/cAMP + ATP ratio, or pERK/total ERK ratio.

## RESULTS

*Signaling Efficacy of DOR Ligands*—In a first series of experiments, we sought to establish the signaling profile of peptidic (DPDPE, TIPP, and TICP) and nonpeptidic (SNC-80, morphine, and naltrindole) DOR ligands that would then be tested in BRET assays. Consistent with previous reports (6, 7), ligand efficacy was influenced by the signaling pathway in which drugs were tested (Fig. 1). Naltrindole, classically considered a neutral antagonist (19), was without effect in the ERK cascade but displayed partial efficacy in the cAMP pathway. DPDPE and SNC-80 inhibited cAMP production and induced ERK phosphorylation, behaving as highly efficacious agonists in both cascades, whereas morphine and TIPP displayed partial efficacy at both readouts. TICP, on the other hand, had a dual profile, sharing agonist capacity to induce ERK activation but opposing agonist ability to inhibit cAMP production. Comparison of ligand rank order of efficacy in cyclase (Fig. 1*A*) and ERK (Fig. 1*B*) cascades also revealed that DOR ligands did not maintain their ordinal positions in the two assays, an observation that has been classically associated with the existence of ligand-specific receptor states (4, 7). We reasoned that if this interpretation of functional data were correct, then DORs occupied by different ligands should distinctively interact with intracellular signaling partners. To assess this possibility, we required an experimental approach that would allow us to monitor DOR interaction with signaling proteins under conditions similar to the ones used in cyclase and mitogen-activated protein kinase readouts. We therefore turned to BRET, since this technology offers the possibility of monitoring protein-protein interactions within living cells.

*Characterization of BRET Constructs and Signal Specificity*—BRET is a naturally occurring phenomenon resulting from the nonradiative transfer of energy between a luminescent donor and a fluorescent acceptor (20). In BRET2 assays, *R*Luc catalyzes oxidation of cell-permeable coelenterazine (DeepBlueC), resulting in luminescence emission within the excitation wavelength of GFP (21). Because the efficacy of energy transfer varies inversely with the sixth power of distance, fluorescence emission by GFP will only take place if donor excitation occurs in close proximity of the acceptor (100 Å). This property may be exploited to monitor interactions between different types of cellular proteins (22, 23), provided that proteins of interest are tagged with donor/acceptor pairs. Increases (decreases) in the BRET signal imply formation (destruction) of new complexes or tags coming closer together (separating) within a preformed complex.

Supplemental Fig. 1*A* shows the different BRET constructs used in this study. Specifically, DOR interaction with the G$\alpha$ subunit was monitored from different vantage points, introducing the acceptor GFP at the receptor C terminus, whereas the donor Luc was inserted at three different locations within the $\alpha_{i1}$ subunit: (i) linker 1 region, which connects helical to GTPase domains ($\alpha_i$-Luc60); (ii) the loop connecting helices $\alpha$A and $\alpha$B of the helical domain ($\alpha_i$-Luc91); and (iii) the loop
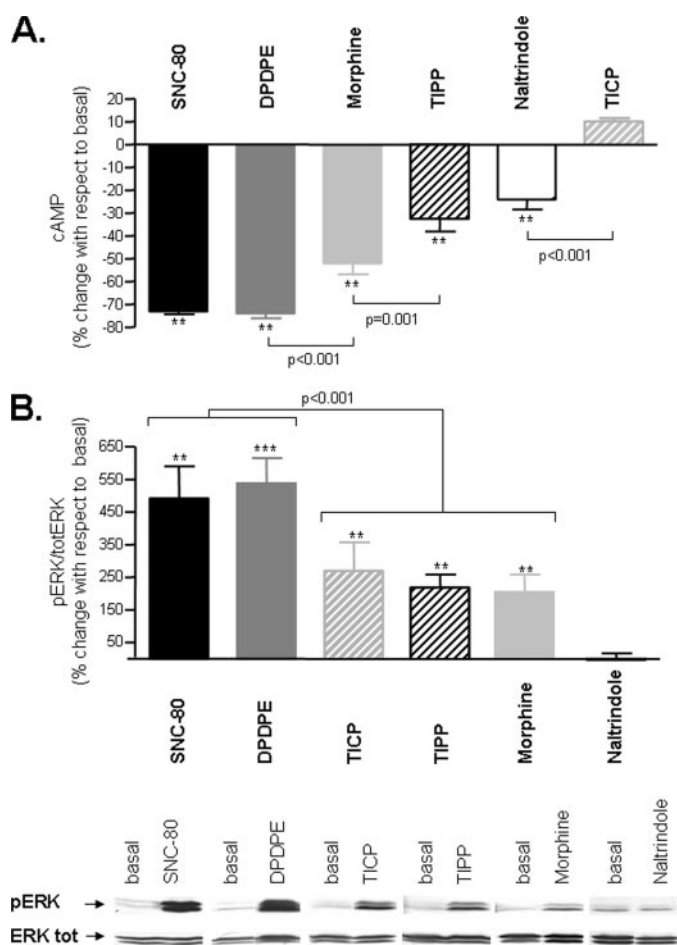
**A.**



**B.**



FIGURE 1. **Functional responses of DOR ligands in adenylyl cyclase and ERK pathways.** *A*, HEK293 cells expressing DOR-FLAG were treated with saturating concentrations (10 $\mu$M) of indicated ligands and cAMP accumulation assays performed in the presence of 25 $\mu$M forskolin as detailed under "Experimental Procedures." Drug effects are expressed as percentage change with respect to the total amount of cAMP produced in the absence of ligand (percentage change in cAMP accumulation = (cAMP$_{ligand}$ − cAMP$_{no\ ligand}$)/cAMP$_{no\ ligand}$ × 100) and correspond to mean ± S.E. of seven experiments carried out in triplicates. *B* (*top*), HEK293 cells expressing DOR-FLAG were exposed to saturating concentrations of the indicated ligands for 5 min, following which ERK signaling was assessed by immunoblot. ERK phosphorylation was normalized to the amount of protein loaded per lane by expressing the data as phospho-ERK/total ERK ratio. Drug effects were expressed as percentage of the basal ratio (percentage of basal = ((pERK/total ERK$_{ligand}$)/(pERK/total ERK$_{no\ ligand}$) × 100)) and represent mean ± S.E. of at least six experiments. *B* (*bottom*), representative immunoblots. pERK and total ERK bands observed in the presence and absence of the indicated drugs. Each drug was paired to its corresponding experimental control from the same blot. To achieve this pairing, lanes containing information not presented in the study were removed by splicing. Examples for different drugs were not necessarily all from the same blot, but they were all matched for total ERK contents and time of film exposure. Statistical analysis is detailed under "Experimental Procedures." *, $p < 0.05$; **, $p < 0.001$.

connecting helices $\alpha$B and $\alpha$C of the same domain ($\alpha_i$-Luc122). Interaction of the G$\beta\gamma$ complex with DORs or $\alpha_{i1}$ subunits was assessed by using DOR-Luc or $\alpha_{i1}$-Luc, respectively, as donors, whereas the acceptor GFP was introduced at the N-terminal domain of $\gamma_2$. The functionality of $\alpha_{i1}$-Luc and GFP-$\gamma_2$ constructs had been previously established (11, 14), and that of receptor fusion proteins was assessed in cAMP assays. As indicated by their ability to support DPDPE-induced inhibition of cAMP production, DOR-GFP and DOR-Luc were functional and adequately expressed at the membrane (supplemental Fig.

1*B*). Their signaling capacity was comparable to that of DOR-FLAG (supplemental Fig. 1*B*), a carboxyl-terminal tagged construct that had been previously shown to be indistinguishable from wild-type DORs (24).

In a first series of BRET assays, DOR-GFP was separately co-expressed with each of the G$\alpha_{i1}$-Luc constructs. Results showed the existence of a spontaneous BRET signal whose magnitude was dependent upon Luc location within the $\alpha$ subunit (Fig. 2*A*). In keeping with these findings, co-immunopurification of DORs with $\alpha_i$-Luc91 or with endogenously expressed $\alpha_{i1}$ subunits showed that the overexpressed $\alpha_{i1}$-Luc construct and the native $\alpha_{i1}$ subunit were both recovered with the receptor (Fig. 2*A*; *inset*), indicating that the spontaneous interaction observed in BRET assays was not due to simultaneous overexpression of the receptor with its G protein signaling partners.

The specificity of the observed interaction between DOR-GFP and $\alpha_{i1}$-Luc was further analyzed in BRET titration assays where donor/acceptor ratios were made to vary by progressively increasing the amount of acceptor constructs (DOR-GFP) available for interaction with a fixed amount of donor ($\alpha_{i1}$-Luc91). Increasing amounts of DOR-GFP efficiently increased energy transfer until reaching a plateau (Fig. 2*B*), an observation consistent with the notion that donor molecules ($\alpha_i$-Luc91) interact with acceptors (DOR-GFP) until reaching saturation (25). In contrast, co-transfection of $\alpha_i$-Luc91 with increasing amounts of a CD8-GFP construct which has similar distribution as the receptor but does not interact with G$\alpha$ (11) (14), produced marginal transfer of energy that did not follow saturation kinetics. In addition, the fact that the highly efficacious DOR agonist SNC-80 (10 $\mu$M; 2 min) modified BRET generated by DOR-GFP·$\alpha_{i1}$-Luc91 but not that corresponding to CD8-GFP, further indicates that the spontaneous transfer of energy obtained by co-expressing DOR·$\alpha_{i1}$ pairs was due to their specific interaction and not simply to their overexpression. It should be noted that BRET does not allow us to identify the exact subcellular localization of interacting proteins, but the signal generated by DOR·$\alpha_{i1}$ BRET pairs most likely represents membrane as well as intracellular complexes in their way to the cell surface.

BRET assays also revealed a spontaneous *in vivo* interaction between DORs and the $\beta\gamma$ complex as well as among $\alpha_{i1}$ and $\beta\gamma$ subunits of the heterotrimeric G protein (Fig. 2*C*). Constitutive association between DORs and the $\beta$ component of the $\beta\gamma$ dimmer was corroborated in immunopurification assays where endogenous and overexpressed $\beta1$ subunits were recovered with the receptor (Fig. 2*C*, *inset*). Specificity of DOR-Luc·GFP-$\gamma_2$ interaction was confirmed in titration assays (Fig. 2*D*) in which this BRET pair was shown to generate a signal that could be saturated and modulated by DOR agonists, whereas coexpression of CD8-Luc with GFP-$\gamma_2$ yielded a low, nonsaturating energy transfer that was unaffected by the presence of SNC-80.

The generation of a constitutive BRET signal among DOR and $\alpha\beta\gamma$ constructs is consistent with the increasingly accepted notion that heptahelical receptors form part of constitutive multiprotein complexes containing transducers, effectors, and regulators of G protein signaling (26). In the next series of
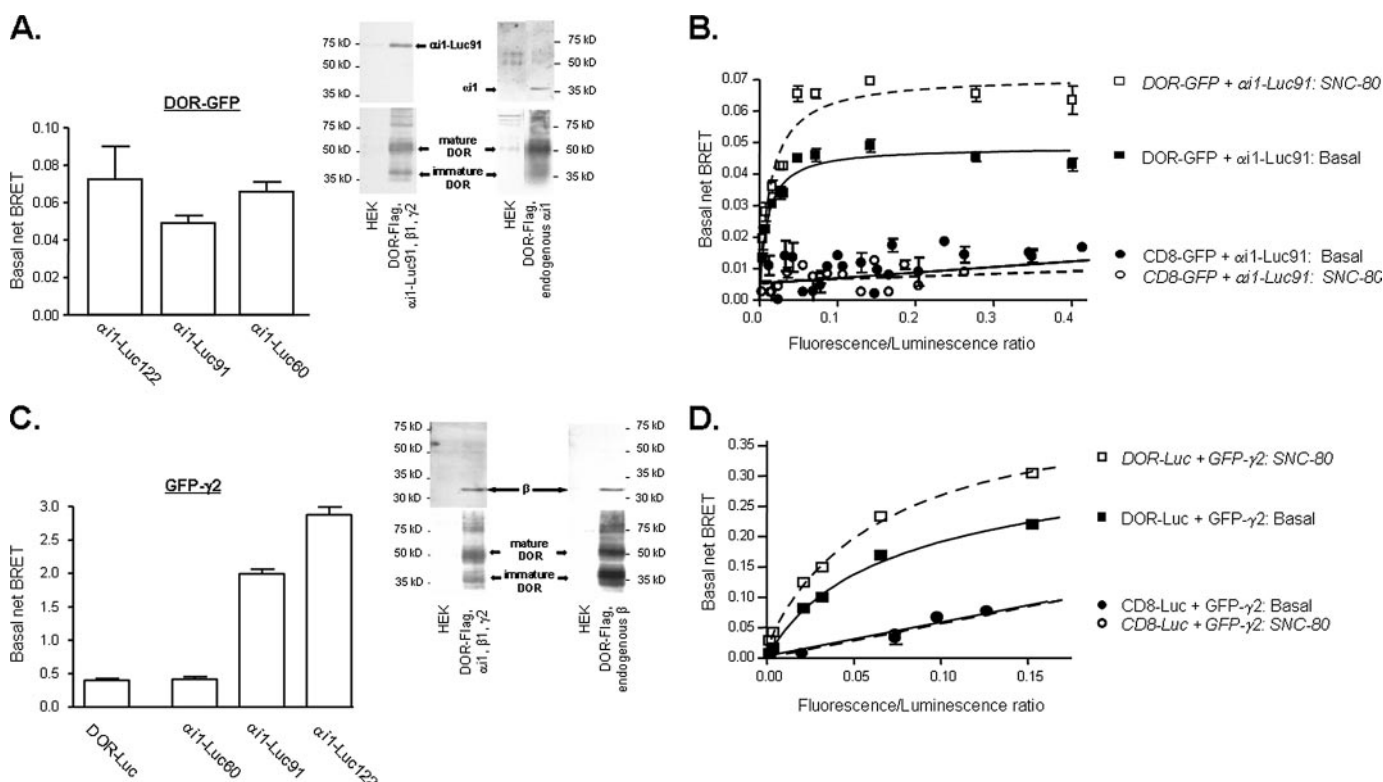
FIGURE 2. **Spontaneous signals generated by different BRET pairs.** *A*, HEK 293 cells were transfected with recombinant plasmids for DOR-GFP, the indicated $\alpha_{i1}$-Luc constructs, and untagged $\beta_1\gamma_2$ subunits. Spontaneous interaction between DORs and $\alpha_{i1}$ subunits was measured by assessing net BRET values in the absence of ligand. Values correspond to mean $\pm$ S.E. of 5–9 experiments carried out in duplicates. *Inset*, HEK 293 cells expressing or not DOR-FLAG were transfected with $\alpha_{i1}$-Luc91$\beta_1\gamma_2$ or vector, and DORs were immunopurified as described under "Experimental Procedures." The amount of $\alpha_{i1}$-Luc91 ($\sim$75 kDa) or endogenous $\alpha_{i1}$ ($\sim$39 kDa) subunits recovered with each purification product was assessed by immunoblot. Results correspond to a representative example of four independent experiments. Blots for $\alpha_{i1}$-Luc91 and endogenous $\alpha_{i1}$ were scanned from separate films. *B*, BRET titration assays were performed by measuring net energy transfer in HEK 293 cells transfected with increasing concentrations of DOR-GFP or CD8-GFP and a fixed amount of $\alpha_{i1}$-Luc91, in combination with untagged $\beta_1\gamma_2$ subunits. *C*, basal interaction between the $\beta\gamma$ complex and DORs was assessed by measuring the spontaneous BRET signal generated by HEK 293 cells expressing GFP-$\gamma_2$ and DOR-Luc in combination with untagged $\alpha_{i1}$ and $\beta_1$ subunits. Interaction between the $\beta\gamma$ complex and $\alpha_{i1}$ subunits was assessed by co-transfecting $\alpha_{i1}$-Luc60, $\alpha_{i1}$-Luc91, or $\alpha_{i1}$-Luc122 with GFP-$\gamma_2$, $\beta_1$ subunits, and DOR-FLAG into HEK 293 cells. Values correspond to mean $\pm$ S.E. of 4–9 experiments carried out in duplicates. *Inset*, HEK 293 cells expressing or not DOR-FLAG were transfected with $\alpha_{i1}\beta_1\gamma_2$ or vector, and DORs were immunopurified as described under "Experimental Procedures." The amount of endogenous or overexpressed $\beta1$ ($\sim$32 kDa) subunits recovered with each purification product was assessed by immunoblot. Results correspond to a representative example of four independent experiments. *D*, BRET titration assays were performed by measuring net energy transfer in HEK 293 cells transfected with increasing amounts of GFP-$\gamma_2$ and a fixed amount of DOR-Luc or CD8-Luc, in combination with untagged $\alpha_{i1}$ and $\beta_1$ subunits.

experiments, we assessed how ligands with different functional profiles modified the association between the receptor and heterotrimeric components of the complex.

*BRET Changes Induced by DPDPE and TICP Are Consistent with a Conformational Rearrangement of DOR·$\alpha_{i1}\beta_1\gamma_2$ Complexes in Living Cells*—The way in which TICP and DPDPE modified basal BRET values was dependent upon tag position within the different BRET pairs. In the case of DPDPE, short term incubation (2 min) at a maximal effective concentration (10 $\mu$M) caused spontaneous energy transfer between DOR-GFP and $\alpha_{i1}$-Luc to be increased at $\alpha_{i1}$-Luc91 but reduced at the construct baring Luc at position 122 (Fig. 3*A*). DPDPE also increased energy transfer at DOR-Luc·GFP-$\gamma_2$ (Fig. 3*B*) and $\alpha_{i1}$-Luc60·GFP-$\gamma_2$ (Fig. 3*C*) while reducing the signal at $\alpha_{i1}$-Luc91·GFP-$\gamma_2$ and $\alpha_{i1}$-Luc122·GFP-$\gamma_2$ (Fig. 3*C*). Given the position of donor/acceptor moieties within each of the BRET constructs, these observations indicate that DPDPE binding caused the accumulation of a receptor species in which the receptor C terminus is closer to the N terminus of $\gamma_2$ than in the unstimulated state. At the same time, while approaching the linker 1 region ($\alpha_i$-Luc60) and the loop connecting helices

$\alpha$A-$\alpha$B of $\alpha_{i1}$ ($\alpha_i$-Luc91), the C terminus of this agonist-activated receptor state separates from the loop connecting helices $\alpha$B and $\alpha$C ($\alpha_i$-Luc122) of the same subunit. DPDPE binding also modified the interaction between $\alpha$ subunit and $\beta\gamma$ complex, bringing the N-terminal region of $\gamma_2$ closer to the linker 1 region but separating it from the loops connecting helices $\alpha$A-$\alpha$B and $\alpha$B-$\alpha$C. As a whole, these BRET changes are better explained by a conformational reorganization of the constitutive signaling complex formed by the receptor and the heterotrimeric subunits than by a change in the absolute number of complexes (11, 27). The propensity of two proteins to form and/or remain in a complex may also be estimated by BRET50 values (25). Hence, the fact that DPDPE did not modify BRET50 for DOR-GFP·$\alpha_{i1}$-Luc91 or DOR-Luc·GFP-$\gamma_2$ (Fig. 3*D*) further supported the notion that agonist binding did not modify the absolute number of DORs interacting with G proteins.

These observations contrast with accepted models of G protein activation, which predict recruitment of G proteins to agonist-occupied receptors and the subsequent dissociation of the $\alpha\beta\gamma$ trimer upon activation (28, 29). Divergence between BRET results and predictions of currently accepted theoretical mod-
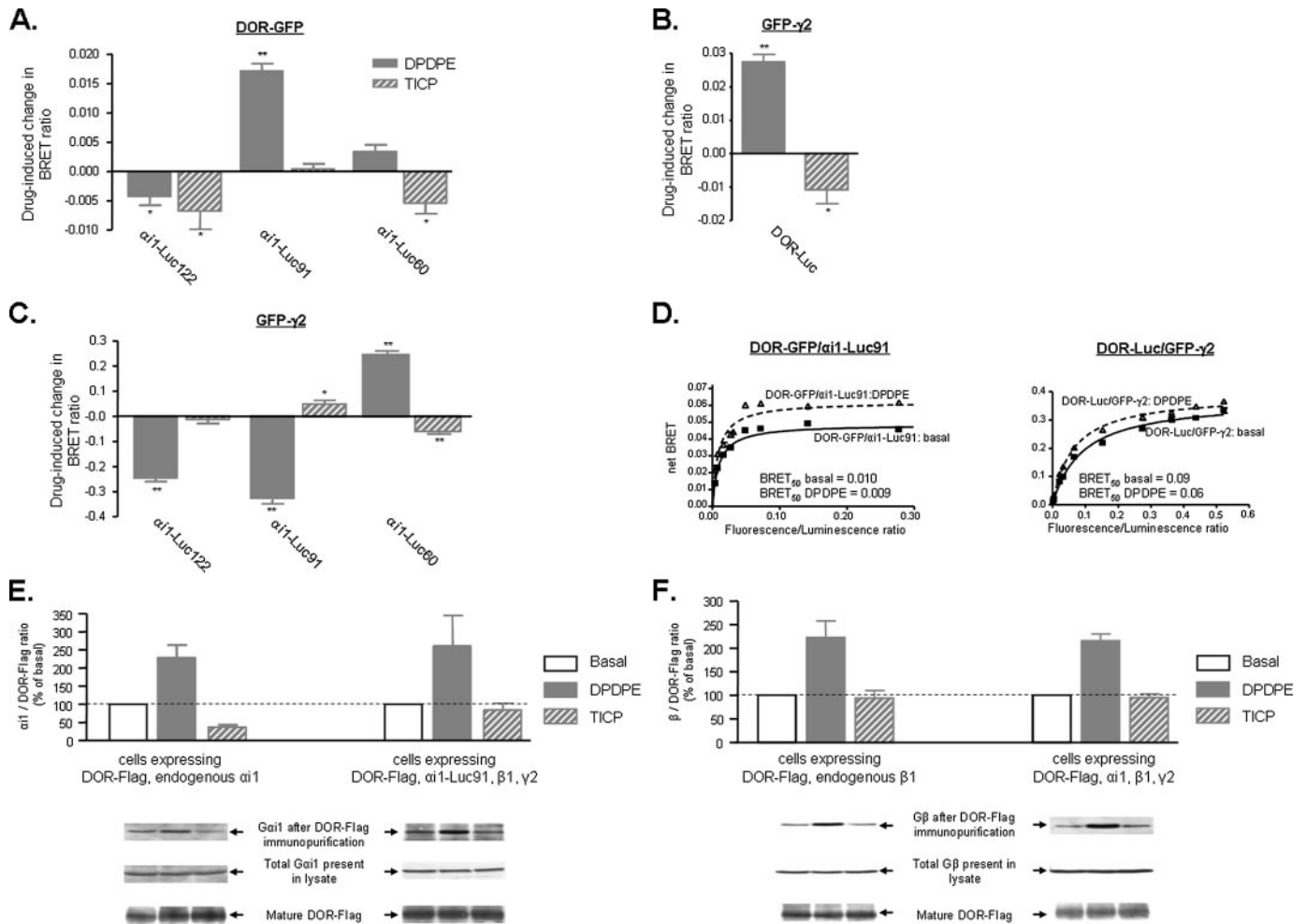
FIGURE 3. **BRET changes promoted by DPDPE and TICP are consistent with conformational reorganization of preformed DOR·$\alpha_{i1}\beta_1\gamma_2$ complexes.** HEK 293 cells were transfected as in Fig. 2, and net BRET signals generated by DOR-GFP and specified $\alpha_{i1}$-Luc partners (*A*), GFP-$\gamma_2$ and DOR-Luc (*B*), or GFP-$\gamma_2$ and specified $\alpha_{i1}$-Luc constructs (*C*) were assessed in the presence or absence of DPDPE or TICP (10 $\mu$M; 2 min). Results were expressed as the difference between measures obtained in the presence or absence of ligand and correspond to mean ± S.E. of at least six experiments carried out in duplicates. *, $p < 0.05$; **, $p < 0.01$. *D*, BRET titration assays were carried out as in Fig. 2, in the presence or absence of DPDPE. BRET50 values represent the calculated ratio of donor/acceptor molecules producing 50% of the energy transfer observed at saturation. *E*, following transfection with DOR-FLAG, $\alpha_{i1}$-Luc91, or vector, in combination with $\beta_1\gamma_2$, cells were exposed or not to DPDPE or TICP as above. Following treatment, receptors were immunopurified, and the product was separated by SDS-PAGE. The amount of $\alpha_{i1}$-Luc91 or endogenous $\alpha_{i1}$ subunits recovered with the receptor was then assessed by immunoblot. DOR interaction with transfected or endogenous $\alpha_{i1}$ subunits was assessed by calculating the immunoreactivity ratio $\alpha_{i1}$/FLAG present in each sample. Results were expressed as percentage of basal values and represent mean ± S.E. of four experiments. Blots for $\alpha_{i1}$-Luc91 and endogenous $\alpha_{i1}$ were scanned from separate films. *F*, cells stably expressing DOR-FLAG were transfected with $\alpha_{i1}\beta_1\gamma_2$ or vector and exposed or not to DPDPE or TICP. Following DOR immunopurification, the amount of endogenous or overexpressed $\beta_1$ subunits recovered with the receptor was assessed by immunoblot. Results are expressed as in *E* and correspond to four experiments. Blots for endogenous and overexpressed $\beta_1$ subunits were scanned from separate films.

els could be related to the fact that BRET monitors receptor-G protein interaction *in vivo*, whereas the prevailing conceptual framework has been largely constructed upon structural and *in vitro* data. Hence, it was of interest to assess how exposure to DPDPE similar to the one used in BRET assays would modify DOR-G protein interaction as monitored by an *in vitro* assay. To do so, cells were exposed to the agonist *in vivo*, and the amount of $\alpha_{i1}$ and $\beta$ subunits recovered with immunopurified DORs was measured by Western blot analysis. As shown in Fig. 3*E*, agonist treatment increased bands corresponding to $\alpha_{i1}$-Luc91 or endogenous $\alpha_{i1}$ immunoreactivity. Similarly, the agonist increased the amount of endogenous or overexpressed $\beta$ subunits that co-purified with the receptor (Fig. 3*F*). Both observations are consistent with formation of new DOR·G protein complexes or with an increase in stability of preexisting ones, but only the latter are compatible with *in vivo* BRET data.

DPDPE and TICP shared an agonistic functional profile when both compounds were tested in the ERK cascade but had opposing actions in the cyclase pathway (Fig. 1). Hence, it was of interest to determine whether these distinct functional phenotypes would be associated with different BRET profiles. Incubation with TICP (10 $\mu$M, 2 min) reduced energy transfer at (i) DOR-GFP·$\alpha_{i1}$-Luc pairs baring tags at positions 60 and 122 (Fig. 3*A*), (ii) the BRET pair evaluating DOR interaction with the $\beta\gamma$ complex (DOR-Luc·$\gamma_2$-GFP; Fig. 3*B*), and (iii) one of the BRET pairs monitoring $\alpha\beta\gamma$ interactions (DOR GFP-$\gamma_2$·$\alpha_{i1}$-Luc60; Fig. 3*C*). At the same time, TICP produced no significant changes in energy transfer at $\gamma_2$-GFP·$\alpha_{i1}$-Luc122 (Fig. 3*C*) or DOR-GFP·$\alpha_{i1}$-Luc91 (Fig. 3*A*) and increased BRET between this same donor and GFP-$\gamma_2$ (Fig. 3*C*). TICP-induced increases and decreases in energy transfer were determined by tag position within different BRET pairs, indicating that, similar to
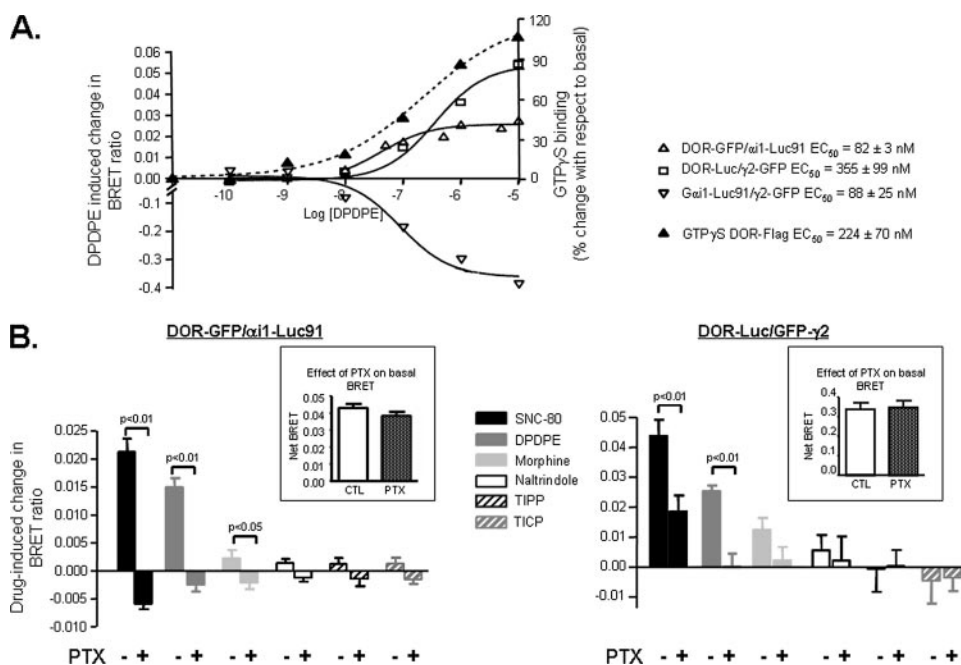
**FIGURE 4. Ligand-promoted BRET changes are associated with G protein activation.** *A*, HEK 293 cells were transiently transfected with the indicated BRET constructs and complementary heterotrimeric subunits and exposed to increasing concentrations of DPDPE to establish dose-response curves at each of the donor/acceptor pairs. Results are expressed as the difference of BRET ratios obtained in presence and absence of drug and are represented in the *left y axis*. The effect of increasing concentrations of DPDPE on G protein activation was assessed by [$^{35}$S]GTP$\gamma$S binding in cells transfected with FLAG-tagged-DORs. Results are expressed as percentage change with respect to basal and are represented on the *right axis*. *B*, cells expressing DOR-GFP·$\alpha_{i1}$-Luc91 ($n = 5–6$) or DOR-Luc·GFP-$\gamma_2$ ($n = 5–6$) were exposed or not to PTX as indicated in the figure (100 ng/ml; 16 h), following which ligand-promoted BRET changes were assessed. *Inset*, net BRET values obtained in controls and PTX-treated cells.

where TICP and DPDPE, respectively, approached and separated GFP-$\gamma_2$ and $\alpha_{i1}$-Luc122 tags.

*Ligand-induced Changes in BRET Are Associated with G$\alpha_i$ Activation—* Dose-response curves for DPDPE showed that this agonist modified BRET signals generated by DOR-GFP·$\alpha_{i1}$-Luc91, DOR-Luc·GFP-$\gamma_2$, and $\alpha_{i1}$-Luc91·GFP-$\gamma_2$ in a concentration-dependent manner and that EC$_{50}$ values at each of these BRET pairs were less than one logarithm apart (Fig. 4A). DPDPE potency to modify energy transfer was also compared with agonist potency to promote G protein activation, revealing that EC$_{50}$ at the different BRET pairs was within the same range as agonist potency to promote [$^{35}$S]GTP$\gamma$S binding (Fig. 4A). This observation suggests a direct link between agonist-induced conformational reorganization of the DOR·G protein complex and activation of the heterotrimer. Moreover, DPDPE potency to modify energy transfer at the different BRET pairs was in better agreement with its potency to promote [$^{35}$S]GTP$\gamma$S

binding (EC$_{50}$ = 224 ± 70 nM; Fig. 4A) than its potency to induce cyclase inhibition (EC$_{50}$ = 7.4 ± 0.6 nM; supplemental Fig. 1), most probably reflecting a lack of amplification between conformational changes revealed by BRET and G protein activation.

An association between ligand-induced changes in energy transfer and G protein activity was further supported by experiments in which BRET assays were performed following exposure to PTX. Indeed, G protein inactivation by the toxin interfered with BRET changes at pairs evaluating DOR interaction with the $\alpha_{i1}$ subunit and the $\beta\gamma$ complex. This effect was particularly evident for ligands displaying high agonist efficacy both at cAMP and ERK readouts (Fig. 4B). In contrast, inactivation of the $\alpha_i$ subunit did not modify the basal BRET signal (Fig. 4B, *insets*), indicating that spontaneous energy transfer was not a consequence of constitutive G protein activation.

*Ligand Rank Order of Efficacy to Modify Energy Transfer Was Not Maintained across All BRET Pairs Tested—*DPDPE and TICP imposed different conformational changes upon the DOR·G protein complex (Fig. 3, *A–C*), indicating that these ligands stabilized different receptor states. However, these observations by themselves do not allow us to conclude whether DORs are stabilized in multiple, ligand-specific conformations (2, 30) or if these BRET changes were the consequence of DPDPE and TICP imposing opposite shifts in the equilibrium between two receptor species (31). To distinguish between these two possibilities, it was necessary

DPDPE, the dual efficacy ligand did not modify the number of DOR $\alpha_{i1}\beta_1\gamma_2$ complexes. In keeping with this notion, BRET50 values for the DOR-Luc·$\alpha_{i1}$-Luc91 pair were not modified by TICP treatment (BRET50 control, 0.011 ± 0.002; BRET50 TICP, 0.010 ± 0.002). Moreover, immunopurification assays indicated that TICP modified the amount of neither endogenous nor overexpressed $\beta$ subunits recovered with the receptor (Fig. 3F), indicating that binding of this ligand did not disrupt DOR-$\beta$ interaction. Although similar results were obtained when evaluating how TICP modified recovery of overexpressed $\alpha_{i1}$ subunits with immunopurified DORs, the observation that the amounts of endogenous $\alpha_{i1}$ subunits recovered with the receptor were reduced by treatment with this ligand suggests a possible reduction in the stability of the DOR-$\alpha_{i1}$ interaction.

TICP and DPDPE induced different changes in basal BRET at six of the seven pairs tested. At four of these pairs, the effects of DPDPE were of opposite direction as those induced by TICP. Donor/acceptors at which these opposing changes took place indicate that both drugs differed in the way they modified DOR interaction with the $\alpha$ subunit (DOR-GFP·$\alpha_{i1}$-Luc60; Fig. 3A) and $\beta\gamma$ complex (DOR-Luc·GFP-$\gamma_2$; Fig. 3B). Furthermore, these differences were carried over to the way $\alpha$ and $\beta\gamma$ subunits positioned themselves with respect to each other, since TICP caused the N-terminal domain of $\gamma_2$ to separate from $\alpha_{i1}$ at the linker 1 region, whereas DPDPE caused the same sites on the two subunits to become closer to one another ($\alpha_{i1}$-Luc60·GFP-$\gamma_2$; Fig. 3C). Divergences between the effects of both drugs were also observed for the $\alpha_{i1}$-Luc122·GFP-$\gamma_2$ pair,
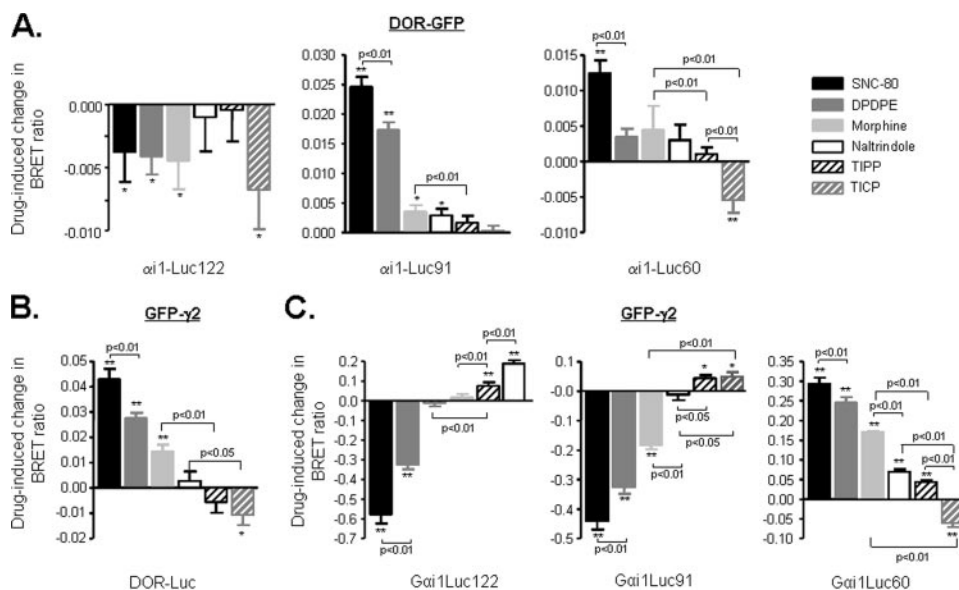
FIGURE 5. **Comparison of ligand-induced BRET changes across different donor/acceptor pairs.** HEK 293 cells were transfected as detailed in previous figures, and BRET signals generated by DOR-GFP and specified $\alpha_{i1}$-Luc partners (*A*) were obtained in the absence and presence of the indicated ligands (10 $\mu$M; 2-min exposure). Results are expressed as the difference between measurements obtained in the presence and absence of ligand and correspond to mean $\pm$ S.E. of 5–9 experiments carried out in duplicates. BRET changes were promoted by different DOR ligands in cells expressing DOR-Luc·GFP-$\gamma_2$ (*n* = 5–7) (*B*) and in cells expressing GFP-$\gamma_2$ and specified $\alpha_{i1}$-Luc partners (*n* = 6) (*C*). Note that DPDPE and TICP results that appear in Fig. 3 were included here for comparison. *, *p* < 0.05; **, *p* < 0.01.

ing ordinal positions to modify basal energy transfer across all BRET pairs, with the exception of DOR-GFP·$\alpha_{i1}$-Luc122 (Fig. 5*A*), where none of the drugs tested differed in their ability to modify basal BRET. Unlike highly efficacious ligands, energy transfer by morphine, TIPP, naltrindole, and TICP was observed only at some of the pairs tested (Fig. 5, *B* and *C*). However, careful analysis of BRET pairs at which energy transfer by these drugs significantly differed from one another indicated that rank order of efficacy was not maintained. Indeed, naltrindole preceded TIPP and TICP at GFP-$\gamma_2$·DOR, GFP-$\gamma_2$·$\alpha_{i1}$-Luc60, and GFP-$\gamma_2$·$\alpha_{i1}$-Luc91 but followed both drugs at GFP-$\gamma_2$·$\alpha_{i1}$-Luc122. Similarly, TIPP preceded TICP at GFP-$\gamma_2$·$\alpha_{i1}$-Luc60, but the order was reversed at GFP-$\gamma_2$·$\alpha_{i1}$-Luc122. Unlike changes in maximal energy transfer, ligands did not modify basal BRET50 values (see Table 1).

## TABLE 1

**Effect of different DOR ligands on BRET50 values calculated from titration assays carried out in cells expressing DOR-GFP·$\alpha_i$-Luc91 and DOR-Luc·GFP-$\gamma_2$**

| Drugs | DOR-GFP versus $\alpha_{i1}$Luc91 | DOR-Luc versus $\gamma_2$-GFP |
|---|---|---|
| Basal | 0.011 ± 0.002 | 0.083 ± 0.006 |
| DPDPE | 0.009 ± 0.002 | 0.054 ± 0.003 |
| SNC-80 | 0.013 ± 0.002 | 0.058 ± 0.004 |
| Morphine | 0.012 ± 0.002 | 0.069 ± 0.004 |
| TIPP | 0.009 ± 0.001 | 0.066 ± 0.004 |
| TICP | 0.010 ± 0.002 | NA[a] |

[a] Not assessed.

to monitor changes in energy transfer by a larger number of ligands. Theoretically, if the two-state alternative is correct and drugs simply differ in their ability to enrich (or deplete) one conformation over the other, then any group of ligands with different signaling efficacies would be expected to induce a progressive modification of BRET values, corresponding to the accumulation (or depletion) of one of the two conformations. In other words, these ligands should produce progressive BRET changes whose rank order should be maintained across all donor/acceptor pairs tested. Failure to comply with these restrictions would falsify the two-state hypothesis in favor of the existence of ligand-specific conformations.

BRET changes induced by ligands with different signaling efficacies at cAMP and ERK readouts (Fig. 1) were tested at seven different sets of BRET pairs and ordered according to magnitude and direction of maximal energy transfer (Fig. 5), which are the parameters that indicate the degree to which tags present in the different BRET pairs are either brought together or separated following ligand binding to the receptor. SNC-80 and DPDPE were always the most efficacious ligands maintain-

## DISCUSSION

An increasing number of reports indicate that modulation of intracellular signaling pathways through heptahelical (seven-transmembrane) receptors may involve multiple active conformations of the same receptor. However, most of this evidence is based on functional data (3, 4), and physical proof of whether intracellular signaling partners are able to structurally discriminate among ligand-specific receptor states has remained limited. We have previously provided functional support to the idea that $\beta_2$-adrenergic receptors and DORs may be stabilized in ligand-specific states with distinct signaling and regulatory properties (6, 7). Below, we discuss how results obtained in this *in vivo* study of DOR-$\alpha_{i1}\beta_1\gamma_2$ interactions rule out the two-state model and favor the existence of ligand-specific conformations.

Macromolecular complexes containing receptors, $\alpha\beta\gamma$ subunits (11, 27), effectors (32–34), and signaling regulators (35) have been described for numerous seven-transmembrane receptors. In addition, *in vivo* molecular imaging techniques have allowed us to establish that these complexes are preassembled before reaching the membrane (26), where they remain associated during the initial phases of agonist-promoted signal transduction (12, 14, 27, 36). Several of our observations are consistent with this notion, since they can only be explained by the existence of constitutive DOR·G protein complexes whose number is not modified by short term exposure to different ligands. Indeed, a spontaneous interaction between DORs and different subunits of heterotrimeric G proteins is supported not only by the existence of a specific basal BRET signal at pairs evaluating DOR-$\alpha_{i1}$, DOR-$\beta_1\gamma_2$, and $\alpha_{i1}$-$\beta_1\gamma_2$ interaction but also by reduction of these signals following

binding of some of the ligands tested. The constitutive association of DORs with the $\alpha_{i1}$ subunit and $\beta\gamma$ complex is further reinforced by *in vitro* results showing that receptors and endogenous or overexpressed $\alpha_{i1}$ and $\beta_1$ subunits were co-immunopurified from untreated cells. In fact, in the case of the $\beta_1$ subunit, its spontaneous association with DORs remained unchanged even following exposure to TICP. Finally, the idea that the total number of DOR·G protein complexes remains constant at early stages of ligand exposure is supported by the observation that a 2-min incubation with different ligands induced position-dependent changes in maximal BRET. Intuitively, this type of observation is better explained by a conformational rearrangement of donor/acceptor tags within a pre-existing complex than by a change in the total number of DORs interacting with G proteins (14). Constant BRET50 values across different treatments are also consistent with this notion. BRET50 is a proximity parameter calculated from experiments in which a fixed amount of donor-tagged proteins is co-expressed with increasing amounts of proteins carrying the acceptor. If energy transfer reaches saturation and the curve is defined by a quadrangular hyperbola, then BRET50 values correspond to the ratio of donor/acceptor molecules producing 50% of energy transfer observed at maximal saturated BRET (25). By analogy with saturation binding assays, this parameter may be used to estimate the ease with which complexes are formed or destroyed. Hence, the stability of this parameter across all pharmacological treatments reinforces the notion that ligand binding promotes neither complex formation nor disintegration.

However, it is difficult to reconcile BRET results in which ligand binding does not modify the total amount of complexes and *in vitro* data indicating that exposure to DPDPE changes the amount of $\alpha$ and $\beta$ subunits recovered with immunopurified DORs. A possible explanation for this divergence could be related to the nature of protein-protein interactions within multimeric arrays. Specifically, we propose that formation or disintegration of a multimeric complex is not exclusively determined by the propensity of any two of its components to interact with one another but through a network of forces linking all of its constituents. For example, evidence from this and other studies indicates that shortly after ligand binding, heptahelical receptors remain associated with heterotrimeric G proteins (11, 37), G protein subunits remain associated with each other (14, 27, 38) and to effectors (34), and effectors maintain their interaction with receptors (32, 39, 40). Under these circumstances, the common interacting partner (effector) would be able to keep a structured complex and proximity between DORs and heterotrimeric subunits even if ligand binding modifies DOR affinity for G proteins. On the other hand, even if a change in their tendency to interact does not modify the total number of DORs associated with $\alpha\beta\gamma$, it could still modify complex stability. Indeed, if ligand binding changes the affinity with which DOR interacts with the $\alpha$ subunit, it could modify resistance of the complex to detergents and the amount of $\alpha\beta\gamma$ subunits recovered by DOR immunopurification. Thus, considering the proximity of complex components as the result of a network of forces and not simply as a consequence of individual relative affinities provides a plau-

**TABLE 2**
Correlations analysis of ligand-induced-BRET changes at donor/acceptor pairs evaluating interaction with DORs or $\beta\gamma$ complex from different vantage points on the $\alpha$ subunit

|  | $R^2$ | $p$ |
|---|---|---|
| **DOR-GFP and $\alpha_{i1}$-Luc constructs** | | |
| $\alpha_{i1}$-Luc60 *versus* $\alpha_{i1}$-Luc91 | 0.614 | 0.065 |
| $\alpha_{i1}$-Luc60 *versus* $\alpha_{i1}$-Luc122 | 0.134 | 0.476 |
| $\alpha_{i1}$-Luc91 *versus* $\alpha_{i1}$-Luc122 | 0.018 | 0.802 |
| **$\gamma_2$-GFP and $\alpha_{i1}$Luc constructs** | | |
| $\alpha_{i1}$-Luc60 *versus* $\alpha_{i1}$-Luc91 | 0.916 | 0.003 |
| $\alpha_{i1}$-Luc60 *versus* $\alpha_{i1}$-Luc122 | 0.554 | 0.090 |
| $\alpha_{i1}$-Luc91 *versus* $\alpha_{i1}$-Luc122 | 0.774 | 0.021 |

**TABLE 3**
Correlation analysis of ligand-induced BRET changes at donor/acceptor pairs monitoring conformational information transferred from the receptor to $\alpha$ subunits and from $\alpha$ subunits to the $\beta\gamma$ complex

|  | $R^2$ | $p$ |
|---|---|---|
| **Correlation for DOR-GFP·$\alpha_i$-Luc60 and $\alpha_i$-Lucs·$\gamma_2$-GFP pairs** | | |
| $\alpha_{i1}$-Luc60·$\gamma_2$-GFP | 0.712 | 0.035 |
| $\alpha_{i1}$-Luc91·$\gamma_2$-GFP | 0.614 | 0.065 |
| $\alpha_{i1}$-Luc122·$\gamma_2$-GFP | 0.400 | 0.178 |
| **Correlation for DOR-GFP·$\alpha_i$-Luc91 and $\alpha_i$-Luc·$\gamma_2$-GFP pairs** | | |
| $\alpha_{i1}$-Luc60·$\gamma_2$-GFP | 0.767 | 0.022 |
| $\alpha_{i1}$-Luc91·$\gamma_2$-GFP | 0.886 | 0.005 |
| $\alpha_{i1}$-Luc122·$\gamma_2$-GFP | 0.866 | 0.007 |
| **Correlation for DOR-GFP·$\alpha_i$-Luc122 and $\alpha_i$-Luc·$\gamma_2$-GFP pairs** | | |
| $\alpha_{i1}$-Luc60·$\gamma_2$-GFP | 0.000 | 0.969 |
| $\alpha_{i1}$-Luc91·$\gamma_2$-GFP | 0.064 | 0.629 |
| $\alpha_{i1}$-Luc122·$\gamma_2$-GFP | 0.109 | 0.523 |

**TABLE 4**
Correlation analysis of ligand-induced change at BRET pairs evaluating conformational change within the G protein heterotrimers and ligand efficacy to induce modulation of cAMP accumulation and ERK phosphorylation

|  | $R^2$ | $p$ |
|---|---|---|
| **Correlation for cAMP signaling and $\alpha_i$Luc·$\gamma2$-GFP constructs** | | |
| $\alpha_{i1}$-Luc60·$\gamma_2$-GFP | 0.954 | 0.008 |
| $\alpha_{i1}$-Luc91·$\gamma_2$-GFP | 0.798 | 0.017 |
| $\alpha_{i1}$-Luc122·$\gamma_2$-GFP | 0.442 | 0.150 |
| **Correlation for ERK signaling and $\alpha_i$Luc·$\gamma2$-GFP constructs** | | |
| $\alpha_{i1}$-Luc60·$\gamma_2$-GFP | 0.344 | 0.226 |
| $\alpha_{i1}$-Luc91·$\gamma_2$-GFP | 0.507 | 0.112 |
| $\alpha_{i1}$-Luc122·$\gamma_2$-GFP | 0.659 | 0.049 |

sible explanation to the observed divergence between BRET and immunopurification data.

Apart from DPDPE and TICP, BRET changes by SNC-80, morphine, TIPP, and naltrindole were also compatible with a conformational rearrangement of the constitutive DOR-G protein complex. Overall, changes in energy transfer induced by the complete series of tested compounds were characterized by differences in magnitude and direction and by a failure to maintain the same rank order of efficacy across the different interactions tested. The latter observation is particularly relevant, because it falsifies the notion that DOR ligands produce differential accumulation of a single active receptor state. Indeed, if the only difference among the tested drugs were their ability to shift equilibrium between two receptor species (active and inactive), then one would expect the increasing ability of differ-
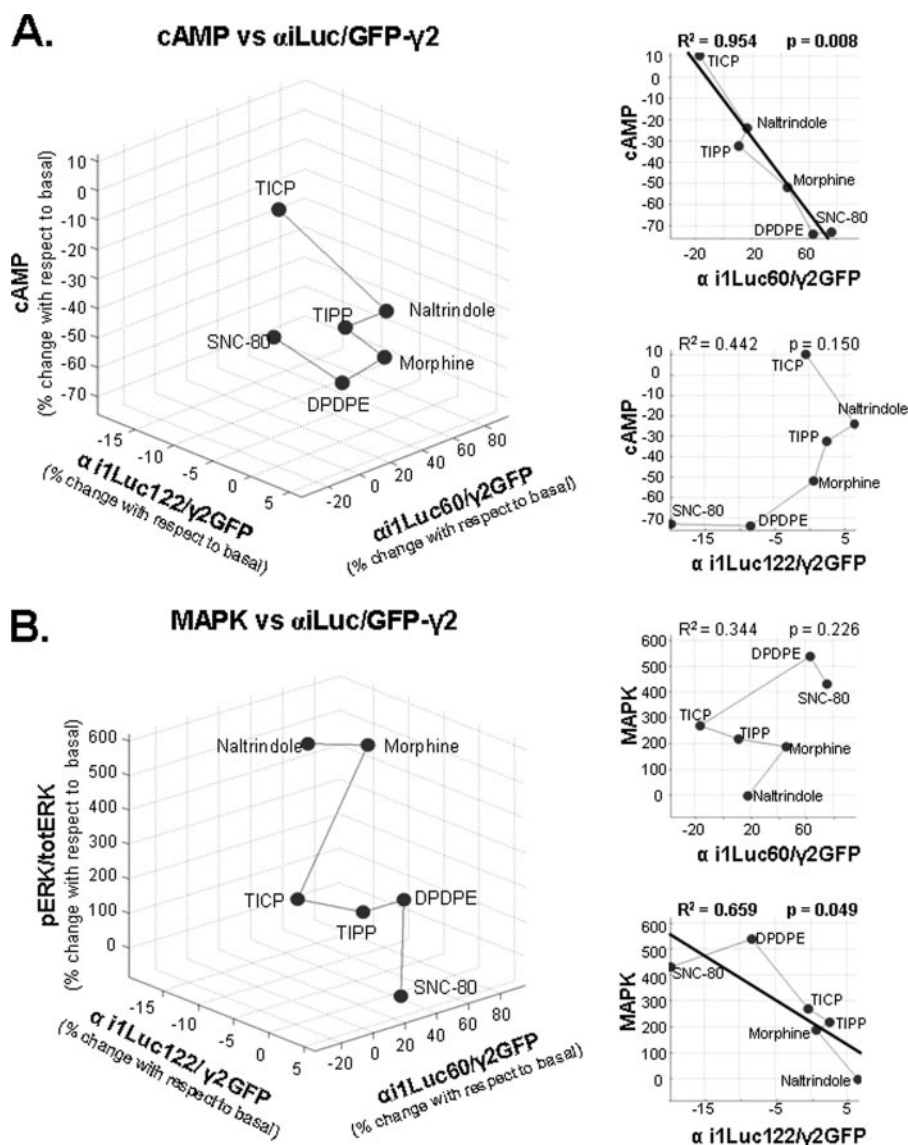
FIGURE 6. **Three-dimensional representations of ligand-induced changes in energy transfer at donor/acceptor pairs monitoring the interaction between αi1-Luc60·GFP-γ2 and αi1-Luc122·GFP-γ2 and ligand efficacy in cAMP assays (*A*) and αi1-Luc60·GFP-γ2 and αi1-Luc122·GFP-γ2, and ligand efficacy in ERK activation assays (*B*).** Points representing different ligands were connected by a *line* that follows their rank order of efficacy in respective functional assays. *Insets* to the *right*, two-dimensional representations for BRET/functional data. *Thick lines* in two-dimensional plots illustrate linear regression for correlated pairs of data sets. Data are expressed as percentage changes with respect to values observed in absence of ligand.

Ligand-induced BRET changes at pairs evaluating DOR interaction with different components of the heterotrimeric G protein were blocked by PTX, and agonist potency to modify energy transfer at these constructs was very similar to $EC_{50}$ values obtained at $[^{35}S]GTP\gamma S$ binding assays. Both of these observations point to a close association between ligand-induced BRET changes and G protein activation (12, 14). Hence, if different ligands were to induce a progressive increase (or depletion) of a unique active receptor conformation, they would also be expected to produce an incremental accumulation (or depletion) of the same active state of the G protein. In other words, one would expect ligand-induced BRET changes at pairs evaluating DOR interaction with different $\alpha_i$-Luc constructs to be correlated with ligand-induced BRET changes at pairs evaluating interaction of the same $\alpha_i$-Luc constructs with the $\beta\gamma$ complex. Table 3 shows the correlation analysis of BRET pairs, assessing how conformational information encoded at DOR-$\alpha_{i1}$ interaction is channeled to $\alpha_{i1}$ interactions with the $\beta\gamma$ complex. The results indicate that ligand-induced BRET changes at DOR interaction with $\alpha_i$-Luc60 or $\alpha_i$-Luc122 were not consistently correlated with downstream conformational changes imposed upon $\alpha_i$-Luc·GFP-$\gamma_2$ pairs following ligand binding to the receptor. Finally, the two-state model would also predict ligand-induced BRET changes at pairs evaluating conformational rearrangement within the G protein heterotrimer to be correlated with DOR ligand efficacy to modify cyclase and mitogen-activated protein kinase signaling, both of which are G protein-dependent (7, 41).[5] Table 4 shows that ligand-induced change in cAMP production or in ERK phosphorylation was not consistently correlated across the different BRET pairs evaluating $\alpha\beta\gamma$ interaction. Interestingly, ligand-induced BRET changes at the single BRET pair that did not correlate with cAMP responses ($\alpha_i$-Luc122·GFP-$\gamma_2$) were the only ones to correlate with ligand ability to induce ERK phosphorylation. A three-dimensional representation of the correlation between each of the functional responses and $\alpha\beta\gamma$ interactions as evaluated by $\alpha_i$-Luc122 and the

ent ligands to enrich (or reduce) one of the species at the expense of the other to transpire as correlated, progressive changes in energy transfer at all donor/acceptor pairs tested. Results summarized in Tables 2 and 3 indicate that BRET changes induced by DOR ligands across different interactions within the DOR-G protein complex do not fulfill these expectations. In particular, Table 2 shows correlation analysis for ligand-induced BRET changes at pairs assessing the same protein-protein interaction from different vantage points (*i.e.* DORs with different $\alpha_i$-Luc constructs or $\beta\gamma$ complex with different $\alpha_i$-Luc constructs). The fact that noncorrelated changes could be detected at both sets of interactions is inconsistent with a two-state model and favors an alternative view in which not only the receptor but heterotrimeric subunits may adopt ligand-specific conformations.

within the G protein heterotrimer to be correlated with DOR ligand efficacy to modify cyclase and mitogen-activated protein kinase signaling, both of which are G protein-dependent (7, 41).[5] Table 4 shows that ligand-induced change in cAMP production or in ERK phosphorylation was not consistently correlated across the different BRET pairs evaluating $\alpha\beta\gamma$ interaction. Interestingly, ligand-induced BRET changes at the single BRET pair that did not correlate with cAMP responses ($\alpha_i$-Luc122·GFP-$\gamma_2$) were the only ones to correlate with ligand ability to induce ERK phosphorylation. A three-dimensional representation of the correlation between each of the functional responses and $\alpha\beta\gamma$ interactions as evaluated by $\alpha_i$-Luc122 and the

[5] Archer-Lahlou, E., Audet, N., Amraei, M. G., Huard, K., Paquin-Gobeil, M., and Pineyro, G. (2008) *J. Cell. Mol. Med.* 10.1111/j.1582-4934.2008.00308.x.

construct bearing the Luc tag at the linker region ($\alpha_i$-Luc60) are shown in Fig. 6. It is quite remarkable that conformational changes evaluated from each of these positions correlated with just one of the functional responses assessed, as if the ERK effector recognized the $\alpha\beta\gamma$ heterotrimer from the same "perspective" as the tag on position 122, whereas adenylyl cyclase shared its vantage point with the tag on position 60 (as well as position 91; Table 4) This interpretation is consistent with the notion that different effectors interact with very specific residues within the G protein (42, 43) that would not necessarily be equally exposed by conformational changes induced by different ligands.

In conclusion, this study showed that DORs and $\alpha_{i1}\beta_1\gamma_2$ subunits are contained within multimeric signaling complexes and provided evidence indicating that the constitutive association between DORs and G proteins is a viable platform whereby conformational diversity encoded by ligand binding to the receptor may be conveyed to downstream signaling relays. This type of organization adds unprecedented diversity to receptor function and has implications for the way we conceive specificity of signal transduction. In particular, since composition of multiprotein arrays is influenced by factors such as expression levels of interacting partners, the presence of scaffolding proteins (44), and membrane compartmentalization (45), not all signaling complexes harboring a specific receptor would be expected to be the same. Thus, a ligand that preferentially recognizes a receptor conformation within a particular type of signaling complex would confine modulation of receptor signaling to cells that express that specific type of array. Alternatively, stabilization of a conformation that allows activation of a specific subset of complexes containing a definite type of effector would restrict consequences of receptor activation to a distinct signaling pathway and to the vital functions it may regulate. Exploiting this signaling diversity could prove effective in developing therapeutic ligands with reduced side effects.

## REFERENCES

1. Furchgott, R. (1966) *Bull. N Y Acad. Med.* **42,** 996–1006
2. Kenakin, T. (2004) *Trends Pharmacol. Sci.* **25,** 186–192
3. Pineyro, G., and Archer-Lahlou, E. (2007) *Cell. Signal.* **19,** 8–19
4. Urban, J. D., Clarke, W. P., von Zastrow, M., Nichols, D. E., Kobilka, B., Weinstein, H., Javitch, J. A., Roth, B. L., Christopoulos, A., Sexton, P. M., Miller, K. J., Spedding, M., and Mailman, R. B. (2007) *J. Pharmacol. Exp. Ther.* **320,** 1–13
5. Berg, K. A., Maayani, S., Goldfarb, J., Scaramellini, C., Leff, P., and Clarke, W. P. (1998) *Mol. Pharmacol.* **54,** 94–104
6. Azzi, M., Charest, P. G., Angers, S., Rousseau, G., Kohout, T., Bouvier, M., and Pineyro, G. (2003) *Proc. Natl. Acad. Sci. U. S. A.* **100,** 11406–11411
7. Audet, N., Paquin-Gobeil, M., Landry-Paquet, O., Schiller, P. W., and Pineyro, G. (2005) *J. Biol. Chem.* **280,** 7808–7816
8. Ghanouni, P., Gryczynski, Z., Steenhuis, J. J., Lee, T. W., Farrens, D. L., Lakowicz, J. R., and Kobilka, B. K. (2001) *J. Biol. Chem.* **276,** 24433–24436
9. Alves, I. D., Salamon, Z., Varga, E., Yamamura, H. I., Tollin, G., and Hruby, V. J. (2003) *J. Biol. Chem.* **278,** 48890–48897
10. Li, J. H., Han, S. J., Hamdan, F. F., Kim, S. K., Jacobson, K. A., Bloodworth, L. M., Zhang, X., and Wess, J. (2007) *J. Biol. Chem.* **282,** 26284–26293
11. Gales, C., Rebois, R. V., Hogue, M., Trieu, P., Breit, A., Hebert, T. E., and Bouvier, M. (2005) *Nat. Methods* **2,** 177–184
12. Ayoub, M. A., Maurel, D., Binet, V., Fink, M., Prezeau, L., Ansanay, H., and Pin, J. P. (2007) *Mol. Pharmacol.* **71,** 1329–1340
13. Dupre, D. J., Robitaille, M., Ethier, N., Villeneuve, L. R., Mamarbachi, A. M., and Hebert, T. E. (2006) *J. Biol. Chem.* **281,** 34561–34573
14. Gales, C., Van Durm, J. J., Schaak, S., Pontier, S., Percherancier, Y., Audet, M., Paris, H., and Bouvier, M. (2006) *Nat. Struct. Mol. Biol.* **13,** 778–786
15. Schiller, P. W., Weltrowska, G., Berezowska, I., Nguyen, T. M., Wilkes, B. C., Lemieux, C., and Chung, N. N. (1999) *Biopolymers* **51,** 411–425
16. Breit, A., Gagnidze, K., Devi, L. A., Lagace, M., and Bouvier, M. (2006) *Mol. Pharmacol.* **70,** 686–696
17. Pineyro, G., Azzi, M., De Lean, A., Schiller, P., and Bouvier, M. (2001) *Mol. Pharmacol.* **60,** 816–827
18. Pineyro, G., Azzi, M., deLean, A., Schiller, P. W., and Bouvier, M. (2005) *Mol. Pharmacol.* **67,** 336–348
19. Quock, R. M., Burkey, T. H., Varga, E., Hosohata, Y., Hosohata, K., Cowell, S. M., Slate, C. A., Ehlert, F. J., Roeske, W. R., and Yamamura, H. I. (1999) *Pharmacol. Rev.* **51,** 503–532
20. Angers, S., Salahpour, A., Joly, E., Hilairet, S., Chelsky, D., Dennis, M., and Bouvier, M. (2000) *Proc. Natl. Acad. Sci. U. S. A.* **97,** 3684–3689
21. Bertrand, L., Parent, S., Caron, M., Legault, M., Joly, E., Angers, S., Bouvier, M., Brown, M., Houle, B., and Menard, L. (2002) *J. Recept. Signal Transduct. Res.* **22,** 533–541
22. Milligan, G., and Bouvier, M. (2005) *Febs J.* **272,** 2914–2925
23. Marullo, S., and Bouvier, M. (2007) *Trends Pharmacol. Sci.* **28,** 362–365
24. Petaja-Repo, U. E., Hogue, M., Laperriere, A., Walker, P., and Bouvier, M. (2000) *J. Biol. Chem.* **275,** 13727–13736
25. Mercier, J. F., Salahpour, A., Angers, S., Breit, A., and Bouvier, M. (2002) *J. Biol. Chem.* **277,** 44925–44931
26. Dupre, D. J., and Hebert, T. E. (2006) *Cell. Signal.* **18,** 1549–1559
27. Bunemann, M., Frank, M., and Lohse, M. J. (2003) *Proc. Natl. Acad. Sci. U. S. A.* **100,** 16077–16082
28. Gilman, A. G. (1987) *Annu. Rev. Biochem.* **56,** 615–649
29. Bourne, H. R. (1997) *Curr. Opin. Cell Biol.* **9,** 134–142
30. Monod, J., Wyman, J., and Changeux, J. P. (1965) *J. Mol. Biol.* **12,** 88–118
31. Koshland, D. E., Jr., Nemethy, G., and Filmer, D. (1966) *Biochemistry* **5,** 365–385
32. Davare, M. A., Avdonin, V., Hall, D. D., Peden, E. M., Burette, A., Weinberg, R. J., Horne, M. C., Hoshi, T., and Hell, J. W. (2001) *Science* **293,** 98–101
33. Lavine, N., Ethier, N., Oak, J. N., Pei, L., Liu, F., Trieu, P., Rebois, R. V., Bouvier, M., Hebert, T. E., and Van Tol, H. H. (2002) *J. Biol. Chem.* **277,** 46010–46019
34. Rebois, R. V., Robitaille, M., Gales, C., Dupre, D. J., Baragli, A., Trieu, P., Ethier, N., Bouvier, M., and Hebert, T. E. (2006) *J. Cell Sci.* **119,** 2807–2818
35. Abramow-Newerly, M., Roy, A. A., Nunn, C., and Chidiac, P. (2006) *Cell. Signal.* **18,** 579–591
36. Lachance, M., Ethier, N., Wolbring, G., Schnetkamp, P. P., and Hebert, T. E. (1999) *Cell. Signal.* **11,** 523–533
37. Nobles, M., Benians, A., and Tinker, A. (2005) *Proc. Natl. Acad. Sci. U. S. A.* **102,** 18706–18711
38. Frank, M., Thumer, L., Lohse, M. J., and Bunemann, M. (2005) *J. Biol. Chem.* **280,** 24584–24590
39. Roy, A. A., Baragli, A., Bernstein, L. S., Hepler, J. R., Hebert, T. E., and Chidiac, P. (2006) *Cell. Signal.* **18,** 336–348
40. Dupre, D. J., Baragli, A., Rebois, R. V., Ethier, N., and Hebert, T. E. (2007) *Cell. Signal.* **19,** 481–489
41. Selley, D. E., Breivogel, C. S., and Childers, S. R. (1998) *J. Recept. Signal Transduct. Res.* **18,** 25–49
42. Ford, C. E., Skiba, N. P., Bae, H., Daaka, Y., Reuveny, E., Shekter, L. R., Rosal, R., Weng, G., Yang, C. S., Iyengar, R., Miller, R. J., Jan, L. Y., Lefkowitz, R. J., and Hamm, H. E. (1998) *Science* **280,** 1271–1274
43. Sunahara, R. K., Tesmer, J. J., Gilman, A. G., and Sprang, S. R. (1997) *Science* **278,** 1943–1947
44. Kreienkamp, H. J. (2002) *Curr. Opin. Pharmacol.* **2,** 581–586
45. Ostrom, R. S., and Insel, P. A. (2004) *Br. J. Pharmacol.* **143,** 235–245